Conformation and Dynamics of a Left-Handed Z-DNA Hairpin: Studies of d(CGCGCGTTTTCGCGCG) in Solution†

Albert S. Benight,*,‡ Yusen Wang,§ Mohan Amaratunga,‡ Rajagopal Chattopadhyaya,∥ Jeff Henderson,⊥ Sue Hanlon,⊥ and Satoshi Ikuta*,§

Department of Chemistry, University of Illinois at Chicago, Chicago, Illinois 60680, Department of Chemistry, Illinois Institute of Technology, Chicago, Illinois 60616, Department of Chemistry, University of California, Berkeley, California 94720, and Department of Biological Chemistry, University of Illinois College of Medicine, Chicago, Illinois 60612

Received November 15, 1988; Revised Manuscript Received December 28, 1988

ABSTRACT: The physical properties of the DNA oligomer d(CGCGCGTTTTCGCGCG) in solvents containing 4 M $NaClO_4$ and 0.1 M NaCl were investigated by proton NMR, optical melting, and circular dichroism spectroscopy. Results of these investigations are as follows: (i) The DNA hexadecamer exists as a unimolecular hairpin in either high or low salt. (ii) In high salt the stem region of the hairpin is in the left-handed Z conformation. (iii) In either high or low salt, the duplex stem of the hairpin is stabilized against melting by ~40 °C compared to the linear core duplex. The added stability of the hairpin is entropic in origin. (iv) In high salt, as the temperature is elevated, the equilibrium structure of the duplex stem of the hairpin shifts from the Z to the B conformation before melting. (v) In low salt, when the DNA duplex exists in the B conformation, attachment of a T_4 single-strand loop to one end only slightly decreases (by 14%) the correlation time of the CH5–CH6 interproton vector. In high salt, when the DNA duplex exists in the Z conformation, the correlation time of the CH5–CH6 interproton vector decreases by 51%. Since these viscosity-corrected correlation times are taken to be indicators of duplex motions on the nanosecond time scale, this result directly suggests a larger amplitude of these motions is present in the duplex stem of the hairpin when it exists in the Z conformation.

Intramolecular stem–loop or so-called hairpin structures can potentially form on any RNA or DNA strand containing a palindromic or self-complementary nucleotide sequence. Hairpins are common structural elements in tRNA and mRNA and undoubtedly required for proper genetic function (Kleckner et al., 1975; Zurawski et al., 1978; Quigley & Rich, 1976; Kim et al., 1973). DNA sequences with the potential to form hairpins have been found in gene transcription regions and origins of DNA replication (Hobom et al., 1978; Gonzalez et al., 1986; Maniatis et al., 1975; Rosenberg & Court, 1979; Wells et al., 1980; Muller & Fitch, 1982). Induction of hairpin structures at inverted repeats in closed circular plasmid DNAs by the torsional stress associated with negative supercoiling has also been reported (Lilley, 1980; Haniford & Pulleyblank, 1985; Panayotatos & Wells, 1981; Vologodskii et al., 1979). An attractive proposition is that DNA hairpins serve as instrumental structural vehicles involved in the critical positioning of regulatory proteins in phases of transcription and replication. Because of the widely suspected involvement of DNA hairpins in genetic processes in vivo, a large body of literature on the physical characterization of DNA hairpins in vitro has accumulated (Wolk et al., 1988; Xodo et al., 1986, 1988a,b; Antosiewicz et al., 1988; Ikuta et al., 1986; Germann et al., 1985; Wemmer et al., 1985; Summers et al., 1985; Hare & Reid, 1986; Haasnoot et al., 1980, 1983; Nadeau & Gilman 1985; Roy et al., 1986; Marky et al., 1983).

Recently, the first crystal structure of a DNA hairpin, formed by the oligomer d(CGCGCGTTTTCGCGCG), indicated the stem region is in the left-handed Z conformation (Chattopadhyaya et al., 1988). Several published solution studies of alternating purine–pyrimidine DNA oligomers of this type have indicated they can also adopt the Z conformation under high-salt conditions (Germann et al., 1985; Xodo et al., 1988b; Wolk et al., 1988). In the present study, NMR, optical melting, and circular dichroism experiments are used to investigate the structure and dynamics of d(CGCGCGTTTTCGCGCG) in solution. Results complement the crystallographic study of the same DNA and published studies of other similar Z-DNA hairpins and demonstrate in 4 M $NaClO_4$ solution this oligomer also forms a hairpin structure with the stem in the Z conformation.

Materials and Methods

Preparation of DNA Samples

NMR Studies. Synthesis of the two DNA oligomers studied, d(CGCGCGTTTTCGCGCG) and d(CGCGCG), hereafter referred to as $d(CG)_3T_4$ and $d(CG)_3$, was by the phosphotriester method (Tan et al., 1983). Following cleavage from solid support and detritylation, the oligomers were purified according to previously described procedures (Ikuta et al., 1984), lyophilized, and stored at −20 °C. Low-salt samples were prepared by dissolving the dried DNAs in a solution of D_2O containing 0.1 M NaCl and 10 mM $NaHPO_4^-$, pH 6.0. For $d(CG)_3T_4$, 85 OD units (~4.25 mg) was dissolved in 0.3 mL of low salt buffered D_2O solution. For $d(CG)_3$, 73 OD units (~3.6 mg) was dissolved in 0.3 mL of buffered D_2O. High-salt samples were prepared by adding the appropriate amount of dry $NaClO_4$, to make the solvent concentration 4 M, directly to each of the low-salt samples. Final DNA concentrations of $d(CG)_3T_4$ and $d(CG)_3$ were 3.0 mM and 2.7 mM (DNA strands), respectively.

Optical Melting and Circular Dichroism (CD) Studies. Optical melting curves and CD spectra were measured on

†This work was supported by NIH Grant GM39471 (A.S.B. and M.A.), Illinois Division of the American Cancer Society Grant 87-30 (Y.W. and S.I.), and the Research Corporation (S.I.).

*Address correspondence to either author.
‡University of Illinois at Chicago.
§Illinois Institute of Technology.
∥University of California.
⊥University of Illinois College of Medicine.

0006-2960/89/0428-3323$01.50/0

Table I: Summary of Melting Curve and Thermodynamic Parameters

DNA oligomer	solvent	t_m (°C)	T_M^{NMR} (°C)	peak height	ΔH (kcal/mol)	ΔS (eu)[a]
$d(CG)_3$	0.1 M NaCl	43.25		0.052	50[b]	161
$d(CG)_3$	4.0 M $NaClO_4$	24.71		0.051	45	151
$d(CG)_3T_4(CG)_3$	0.1 M NaCl	86.52	87[b]	0.049	50	139
$d(CG)_3T_4(CG)_3$	4.0 M $NaClO_4$	64.08	79[c]	0.050	45	133
standard deviation		±0.2	±1	±0.002	±1.5	±2

[a] Calculated from $\Delta S \cong \Delta H/T_M(K)$. [b] From Ikuta et al. (1986). [c] T_M^{NMR} of protons displaying monophasic transitions.

separately synthesized batches of $d(CG)_3T_4$ and $d(CG)_3$. These samples were synthesized by the phosphotriester method using β-cyanoethyl phosphoramidites (Caruthers, 1982). An Applied Biosystems 380B automated DNA synthesizer was employed. Following solid-support cleavage and detritylation, the DNAs were dried under vacuum and resuspended in 2 mL of doubly distilled H_2O. Analysis of the crude synthetic material on 20% polyacrylamide gels [18.8% acrylamide, 1.2% bis(acrylamide)], under loading conditions where ≥2% contamination from failure sequences could be detected, did not reveal any contamination. The crude synthetic DNAs were therefore solvated in the appropriate buffer solution and used in melting and CD experiments without further purification.

Prior to melting experiments, DNA samples were freshly prepared from a concentrated DNA stock solution (350 μM) that was stored at 4 °C. Approximately 15 μL was removed and diluted ~70-fold in 1 mL of the melting buffer. Concentrations of the final solutions were around 5 μM (DNA strands). Before melting, both the DNA sample and buffer reference were degassed by bubbling with prepurified helium followed by centrifugation at 2000 rpm for 5 min. For concentration-dependent melts of $d(CG)_3$ in 4 M $NaClO_4$, DNA solutions were prepared from the concentrated stock solution at DNA strand concentrations of 1 and 11 μM and melted.

For CD measurements 1 mL of each DNA stock solution was desalted by being run over a C-18 spice cartridge (Rannen Instruments, Woburn, MA). The samples were then vacuum dried and resuspended in the appropriate buffer (high or low salt) to a final DNA strand concentration of 10 μM (A_{260nm} = 1.0). CD spectra were reduced to mean residue ellipticity with units of deg·cm²/dmol of nucleotide.

NMR Measurements

NMR spectra and relaxation data were obtained on a Nicolet NT-300 instrument with a 293-C pulse programmer. Nuclear Overhauser effects (NOE) were recorded by one-dimensional difference spectroscopy at different lengths of time. Cross-relaxation rates were obtained from the buildup rates of the NOE. All experiments were repeated at least twice. Pure absorption-phase NOESY spectra were obtained from 2048 points in t_2 and 256 points in t_1 (States et al., 1982). A total of 64 scans were accumulated with a 3-s delay between acquisitions. Processing of the NOESY data was carried out on a VAX-750 computer employing the HARE analysis program (generously provided by Dr. D. R. Hare). In low salt, chemical shifts (in ppm) were determined relative to the chemical shifts of the residual HOD peak. In high salt, because the HOD peak shifted upfield by ~0.5 ppm, chemical shifts were determined relative to the DSS signal at different temperatures.

Optical Melting Experiments

Melting curves were collected on a Hewlett-Packard 8450A diode array double-beam spectrophotometer equipped with thermostated cell holders. Sample temperature was measured by a Teflon-coated temperature probe immersed directly in the sample cuvette. Quartz cuvettes with a 1-cm path length were used for all melting experiments. Sample and reference temperatures were increased linearly at a rate of 18 °C/h. All melting curves were completely reversible upon cooling at the same rate. Sample temperature and absorbance at 268 nm were measured simultaneously every 18 s (ca. every 0.09 °C) and collected by an IBM-AT personal computer interfaced to the spectrophotometer. Melting curves of $d(CG)_3$ in 4 M $NaClO_4$ were collected at temperatures from 2 to 40 °C. In 0.1 M NaCl a temperature range from 15 to 70 °C was sampled. Melting curves of $d(CG)_3T_4$ in both low and high salt were recorded from 10 to 99 °C. The procedures used in smoothing and analyzing melting data were the same as recently reported (Benight et al., 1988).

Multiple-wavelength absorbance measurements of $d(CG)_3T_4$ as a function of temperature were made in 1 °C increments from 20 to 95 °C. At each temperature the sample and reference were allowed to equilibrate for 30 s before 15 measurements of the entire spectrum from 340 to 220 nm were collected over the next 60 s. The average spectrum of these 15 scans at each temperature provided the desired absorbance values at 295 and 268 nm. The DNA absorbance was monitored at 268 nm for two reasons: (1) the change in extinction coefficient upon melting of G-C or A-T pairs is approximately the same at 268 nm, and thus, the hyperchromicity is independent of sequence bias; (2) 268 nm is close enough to the isosbestic point of the absorbance spectrum of $d(CG)_3T_4$ in low and high salt (265.5 nm) such that absorbance changes monitor only the melting transition and not other structural transitions that occur within the duplex. The DNA absorbance at 295 nm is a well-known spectral characteristic of the Z conformation.

CD Measurements

CD spectra were recorded on a Jasco (Model J40A) spectropolarimeter. Sample temperatures were controlled by a thermostated sample cell. Wavelengths were scanned from 350 to 220 nm at a rate of 5 nm/min. CD spectra at constant temperature were recorded at 20 °C. CD spectra as a function of temperature were collected after the sample was allowed to equilibrate for ~5 min at each temperature from 25 to 75 °C.

RESULTS

d(CGCGCGTTTTCGCGCG) Is a Unimolecular Hairpin. The absorbance at 268 nm versus temperature curves were normalized to upper and lower base lines and differentiated with respect to temperature (Benight et al., 1988). All the differential melting curves displayed a single symmetric peaked (data not shown). The experimental transition temperature t_m and peak height of each differential melting curve are given in Table I. Since the absorbance at 268 nm monitors only the transformation from the duplex to single strands and not other structural transitions such as the B to Z transition (see discussion below on this structural transition), the melting data indicate the melting transitions at DNA strand concentrations around 5 μM are essentially *monophasic* in both high and low salt. Melting curves of $d(CG)_3T_4$ at a 100-fold higher DNA

concentration (~500 μM) were similarly monophasic in high and low salt (data not shown). $d(CG)_3T_4$ melts with a transition temperature t_m = 64.1 °C in high salt and 86.5 °C in low salt. t_m's of $d(CG)_3$ at a 5 μM strand concentration were 24.7 and 43.3 °C in high and low salt, respectively. The t_m's of $d(CG)_3$ in high salt at 1 and 11 μM (DNA strands) were 20.2 and 28.9 °C, respectively. Thus, the addition of a T_4 single-strand loop to the end of a $d(CG)_3$ duplex DNA stabilizes the duplex against melting by approximately 40 °C, regardless of the salt environment. $NaClO_4$ at 4 M destabilizes both $d(CG)_3$ and $d(CG)_3T_4$ by approximately the same amount (~20 °C). An interpretation of these observations can be made on the basis of the thermodynamic parameters of the melting transitions of the hairpins and core duplexes.

For a strictly two-state transition, the transition enthalpy ΔH of $d(CG)_3T_4$ can be evaluated from the van't Hoff relation (Breslauer et al., 1975):

$$\Delta H = 4R(T_m)^2(d\theta/dT)_{max} \quad (1)$$

If other structural transitions involving the duplex form are present, then the transition enthalpy evaluated from eq 1 represents the upper limit on ΔH. From the values of $T_m(K)$ and maximum peak height $(d\theta/dT)_{max}$ given in Table I, the transition enthalpy of $d(CG)_3T_4$ in 0.1 M NaCl was evaluated to be = 50 kcal/mol. In 4 M $NaClO_4$, ΔH = 45 kcal/mol. The transition entropy ΔS for the hairpins can be obtained from ΔH and T_m by

$$\Delta S = \Delta H/T_m \quad (2)$$

ΔS = 139 eu for $d(CG)_3T_4$ in low salt and 133 eu in high salt.

Previously the transition enthalpy of the linear core duplex in 0.1 M NaCl was evaluated to be ΔH = 50 kcal/mol (Ikuta et al., 1986). We performed a van't Hoff analysis to evaluate ΔH of $d(CG)_3$ in 4 M $NaClO_4$. $d(CG)_3$ was melted in 4 M $NaClO_4$ at DNA concentrations C_T ranging from 1 to 11 μM (data not shown). From the slope of the plot of $1/T_m(K)$ versus ln C_T, the transition enthalpy of $d(CG)_3$ in high salt was evaluated (in the standard way; Manzini et al., 1987) to be ΔH = 45 kcal/mol. This value is in close agreement with ΔH = 46 kcal/mol evaluated for $d(CG)_3$ in 5 M NaCl (Manzini et al., 1987), indicating effects of 4 M $NaClO_4$ and 5 M NaCl on ΔH of $d(CG)_3$ are apparently not greatly different when the DNA adopts the Z conformation. The values of ΔS calculated from ΔH and T_m of $d(CG)_3$ are 161 eu in low salt and 151 eu in high salt. ΔH and ΔS for the hairpin and linear core duplex in high and low salt are listed in Table I.

The essentially identical values of ΔH for $d(CG)_3$ and $d(CG)_3T_4$ in both high and low salt confirm, below t_m, $d(CG)_3T_4$ exists in the unimolecular hairpin state in both high- and low-salt solutions and, as temperature is increased, the transition from the unimolecular hairpin to a coiled single strand is monitored by the melting curve. The approximately 20 eu higher transition entropy for $d(CG)_3$ over that for $d(CG)_3T_4$ in both high and low salt as given in Table I further indicates the marked stabilization of the core duplex by the hairpin loop is entropic in origin.

Thermal Behavior of Chemical Shifts. Assignments of the $d(CG)_3T_4$ and $d(CG)_3$ one-dimensional proton NMR spectra in high salt were made by direct comparison with the previously assigned spectrum of $d(CG)_3T_4$ in low salt (Ikuta et al., 1986). Plots of the chemical shifts versus temperature from 2 to 100 °C of the base protons (GH8, TH6, CH6, and CH5) and sugar protons (CH1′ and GH1′) of $d(CG)_3T_4$ at a concentration of 3 mM measured in 4 M $NaClO_4$ are shown in Figure 1. Curves of the type shown in Figure 1 have previously been termed "NMR melting curves" (Wemmer et al., 1985; Petersheim & Turner, 1983).

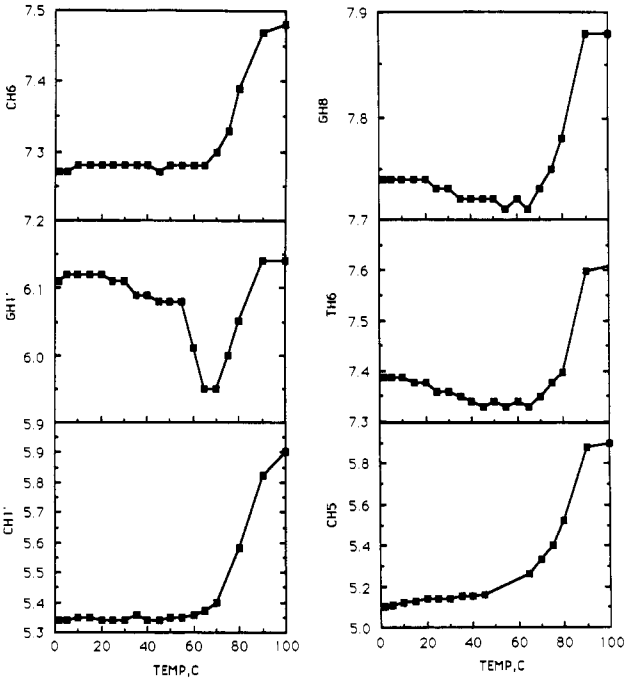

FIGURE 1: Chemical shift melting curves. Chemical shift (ppm) of the aromatic (GH8, TH6, CH6, CH1′, CH5, and GH1′) proton resonances of the hairpin in 4 M $NaClO_4$ versus temperature. The temperature at which half of the total observed chemical shift occurs, T_M^{NMR}, of each proton is ~79 °C. Note the GH1′ proton transition is singularly biphasic.

The proton melting curves depicted in Figure 1, with the exception of the GH1′ curve, display a single transition. The transition temperature T_M^{NMR} of each chemical shift displaying a monophasic transition, estimated as the temperature at which half of the total observed chemical shift occurs, is ~79 °C as given in Table I. Such nearly universal monophasic curves suggest a two-state transition is monitored by these proton chemical shifts. This observation is in direct analogy with the results from the optical melting curve analysis except for the fact that the T_M^{NMR} of the protons (as indicated in Table I) exceeds the optically determined t_m by ~15 °C! As indicated in Table I, this result is in contrast to that found for $d(CG)_3T_4$ in low salt, where the transition temperatures determined from the optical melting curve (this work) and the temperature dependence of the proton chemical shifts (Ikuta et al., 1986) are essentially the same. Such a finding suggests the proton chemical shifts of the hairpin in 4 M $NaClO_4$ are a function of not only the DNA melting transition but other higher temperature transitions as well. One possibility is the single strand maintains sufficient structural features above the melting temperature and the higher temperatures of the chemical shift transitions reflect the stability of the structured single strand. A structured single strand, where the bases preserve some stacking, was proposed to account for the lower than expected activation energy, compared to the melting enthalpy, evaluated for conversion of the self-complementary duplex d(CGCGAATTACGCG) to the unimolecular hairpin (Roy et al., 1986). Beyond this, we cannot presently provide a clearer explanation for the elevated transition temperatures of the chemical shifts. Even so, the "other" transitions monitored by the temperature-dependent chemical shifts do appear to display two-state character, just as observed for the optical melting curves.

Conformation of the Glycosidic Torsion Angle. Results of pre-steady-state NOE experiments conducted on $d(CG)_3T_4$

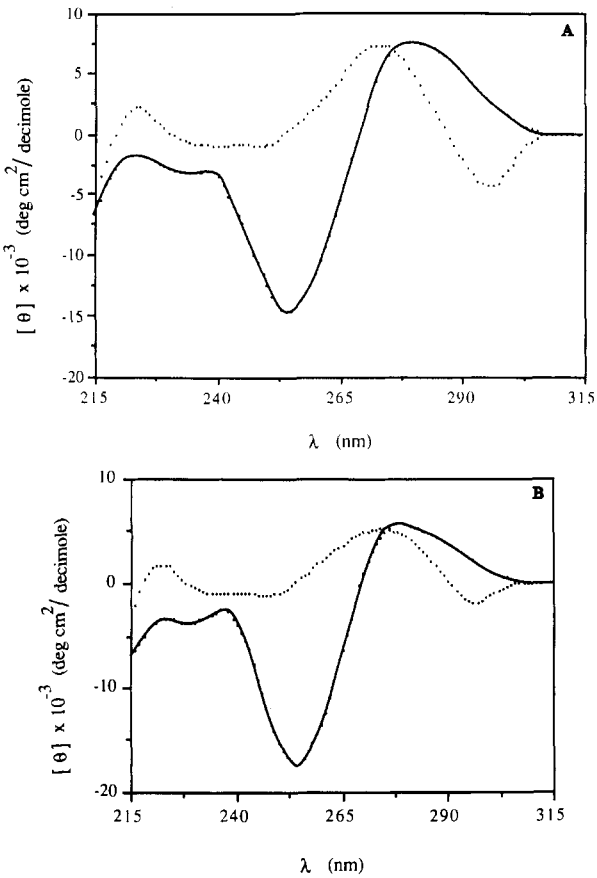

FIGURE 2: (A) Circular dichroism spectra of the hairpin in high and low salt. Ellipticity (θ) in deg-cm^2/dmol is plotted versus wavelength (λ) in nanometers. The solid line is the spectrum in low salt. The dotted line is the high-salt spectrum. Spectra were measured at 20 °C. (b) Circular dichroism spectra of d(CG)$_3$ in high and low salt are plotted as in (A).

in high salt (data not shown) indicated saturation of the GH8 proton resonance at 7.77 ppm results in a large intrabase NOE at 6.19 ppm, the position of the GH1′ sugar proton resonance. Also, a small NOE was observed upfield near 2.5 ppm that corresponds to the H2′ and H2″ resonances. Saturation of the 6.19-ppm GH1′ resonance also resulted in a large NOE at the 7.77-ppm GH8 resonance. The NOE data indicated the GH8 and GH1′ protons reside in close spatial proximity. This is consistent with the conclusion that the guanine residues reside in the syn conformation around the β-glycosidic bond. The syn conformation of guanines is well-known to be diagnostic of Z-DNA (Patel et al., 1982). As described below, CD measurements support this.

CD Spectra. CD spectra of d(CG)$_3$T$_4$ and d(CG)$_3$ recorded at 20 °C in high and low salt are shown in Figure 2. In low salt the CD spectra are very B-like, nearly antisymmetric with a positive peak at 280 nm, negative trough at 255 nm, and cross-over point at 268 nm. In high salt the spectra are inverted, red shifted, and comprised of a negative trough at 296 nm, a positive peak at 275 nm, and cross-over point at 289 nm. These spectral features are well-known to be characteristic of the left-handed Z conformation of poly[d(GC)] DNA (Pohl & Jovin, 1972). These results, in conjunction with the NMR data, indicate that d(CG)$_3$ and d(CG)$_3$T$_4$ adopt the B conformation in low salt and the Z conformation in high salt.

Z to B Transition Equilibrium Is Shifted in Favor of the B Form Prior to the Melting Transition of the Hairpin. As previously noted and indicated in Figure 1, the chemical shift versus temperature curve of the GH1′ proton resonance exhibits singular behavior. Unlike the monophasic temperature-dependent transitions of the chemical shifts of the other protons, the chemical shift curve of the GH1′ proton displays two transitions. The first transition of GH1′ occurs at ~58 °C, approximately 20 °C prior to the higher temperature transition and T_M^{NMR} of the other protons. The chemical shift of the GH1′ is known to be a function of the glycosidic torsion angle (Patel et al., 1982). A transition of the deoxyribose rings relative to the guanine base residues to which they are attached, from the syn to the anti conformation, is consistent with these observations. Thus, it necessarily follows that the lower temperature chemical shift transition of the GH1′ resonance monitors the temperature dependence of the Z to B transition. Absorbance and CD measurements as a function of temperature essentially corroborate this finding.

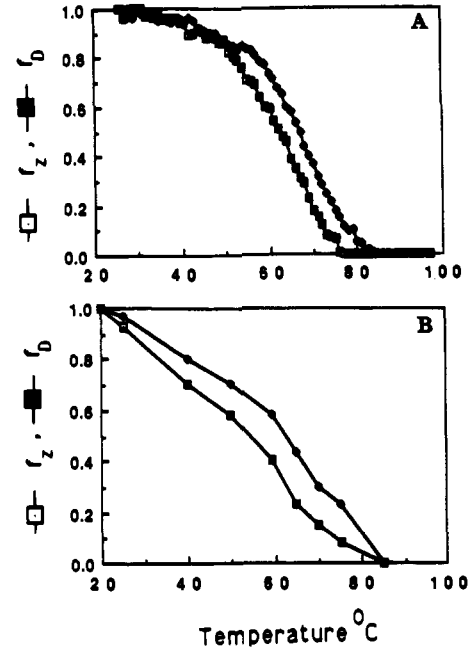

FIGURE 3: Plots of the fraction of hairpin molecules in the Z conformation, f_Z, and fraction of duplex hairpins, f_D, as a function of temperature in high salt: (A) calculated from the temperature dependence of the absorbance at 295 and 268 nm; (B) calculated from a multicomponent linear regression analysis of the CD spectra as a function of temperature. (A) and (B) clearly show the temperature-induced shift of the equilibrium from the Z to the B structure prior to the melting transition.

Plotted in Figure 3A are the fraction of molecules in the Z conformation f_Z and fraction of molecules in the bonded hairpin duplex f_D versus temperature. f_Z was calculated as follows:

$$f_Z = 1 - \{[A_{295}(20\ °C) - A_{295}(T)]/[A_{295}(20\ °C) - A_{295}(95\ °C)]\} \quad (3)$$

where $A_{295}(20\ °C)$ and $A_{295}(95\ °C)$ are the absorbance values at 295 nm at 20 and 95 °C, respectively. $A_{295}(T)$ is the absorbance as a function of temperature T at 295 nm and indicates the relative amount of Z-type structure. The absorbance at 295 nm of d(CG)$_3$T$_4$ in low salt is invariant over the entire transition region (data not shown). f_D was calculated as follows:

$$f_D = 1 - \{[A_{268}(T) - A_{268}(20\ °C)]/[A_{268}(95\ °C) - A_{268}(20\ °C)]\} \quad (4)$$

Similarly, $A_{268}(20\ °C)$ and $A_{268}(95\ °C)$ are the absorbance values at 268 nm at 20 and 95 °C, respectively. $A_{268}(T)$ is the absorbance at 268 nm as a function of temperature. Figure 3A indicates the Z to B transition temperature, when $f_Z = 0.5$, occurs at ~61 °C, 6 °C below the indicated helix to coil

transition temperature of 67 °C where $f_D = 0.5$. These transition temperatures are shifted higher by approximately 3 °C from the values obtained from the proton and optical melting curves probably because base-line corrections have not been performed for each of the curves in Figure 3A. The measured relative difference is the salient feature of these data which indicates a temperature-induced shift in the equilibrium from the Z to the B conformation of $d(CG)_3T_4$.

A further indication that the Z to B transition precedes the helix to coil transition in the hairpin is given in Figure 3B. CD measurements of $d(CG)_3T_4$ in high salt as a function of temperature (data not shown) also indicated the CD spectrum undergoes a progressive inversion away from the Z to the B conformation as temperature is increased. The Z to B transition occurred between 40 and 60 °C.

A plot similar to that obtained from the absorbance behavior as a function of temperature (shown in Figure 3A) can also be calculated from the temperature dependence of the CD spectra. Figure 3B results from a multicomponent linear regression analysis of the CD spectrum at every wavelength over the range from 240 to 305 nm as a function of temperature. Assumptions made in assigning the end-point values for each component were as follows: (1) At 20 °C, the fractions of Z form (f_Z) and duplex form (f_D) were assumed to be 1.0; (2) because technical problems precluded measurement of the CD spectra at 85 °C, the absorbance data at 85 °C indicated the high-temperature end points. These values were then subsequently utilized to calculate the fractional amounts of each component at 75 °C. At every temperature, f_Z (the fraction of Z), f_B (the fraction of B), and $f_{SS} = 1 - f_Z - f_B$ (the fraction of melted single strands) summed to 1. In Figure 3B, $f_Z = 0.5$ at 53 °C and $f_D = f_Z + f_B = 0.5$ at 63 °C. These values are in close agreement with the transition midpoint temperatures obtained from the optical melting curve and the NMR melting curve of the GH1′ resonance shown in Figure 1. Because the spectral analysis is subject to a number of assumptions and constraints, it is not surprising the absolute values of the transition temperatures obtained from the optical absorbance and CD spectra are slightly different. More importantly, as comparison of panels A and B of Figure 3 indicates, essentially the same behavioral trend of the Z hairpin as a function of temperature is revealed by the absorbance and CD measurements.

NMR of the Loop Protons. Two-dimensional NOESY spectra of $d(CG)_3T_4$ in low and high salt were recorded at 5 °C with a mixing time of 200 ms (data not shown). In low salt intense cross peaks between the H6 proton of thymine (TH6) and the methyl group of thymine (T-CH_3) were seen. As was previously noted (Ikuta et al., 1986), one of the T-CH_3 resonances also had a cross peak with one of the GH8 resonances. These two resonances were assigned to the bases T_7 and G_6, respectively (Ikuta et al., 1986).

The NOESY spectra indicated in low salt that the last guanine residue of the stem region before the loop, G_6, is in close contact with the first thymine of the loop, residue T_7. Similar observations were reported for the similar DNA hairpin oligomers $d(CG)_2T_4(CG)_2$ in 10 mM $NaHPO_4^-$ (Hare & Reid, 1986) and $d(CG)_5T_4(CG)_5$ in 0.12 M NaCl (Wolk et al., 1988). Even though the ionic environments are different, the spectrum of $d(CG)_3T_4$ in 0.1 M NaCl strongly resembled that reported for $d(CG)_2T_4(CG)_2$ (Hare & Reid, 1986).

In high salt, the NOESY spectrum was markedly changed from that in low salt. In contrast to the NOE observed between GH8 and T-CH_3 in low salt, an NOE between these protons was not observed in high salt. Absence of this NOE in the high-salt spectrum indicates the base proton, GH8, of the stem and base proton, TH6, of the loop are further apart in high salt when the stem resides in the left-handed Z conformation.

Table II: Cross-Relaxation Rates of the CH5–CH6 Interproton Vector σ_{ij} Measured at 5 °C[a]

DNA oligomer	solvent	σ_{ij} (s^{-1})	τ_c (ns)	$\tau_c(\eta_0/\eta)R$ (ns)
$d(CG)_3T_4(CG)_3$	0.1 M NaCl	0.61	2.54	1.58
$d(CG)_3T_4(CG)_3$	4.0 M $NaClO_4$	0.45	1.96	0.93
$d(CG)_3$	0.1 M NaCl	0.72	2.95	1.85
$d(CG)_3$	4.0 M $NaClO_4$	1.01	4.04	1.91

[a] Apparent correlation times, τ_c, calculated directly from σ_{ij} as given in the text. $\tau_c(\eta_0/\eta)R$ is the viscosity-corrected correlation time. η_0 is the viscosity of water at 20 °C. R is the temperature ratio = 278.15 K/293.15 K = 0.95.

Correlation Times of the CH5–CH6 Interproton Vector. A series of pre-steady-state NOE measurements were made on $d(CG)_3T_4$ and $d(CG)_3$ in high and low salt for irradiation times ranging from 50 to 200 ms. The methods employed were essentially those previously reported (Clore & Gronenborn, 1984). Following saturation of the CH6 resonance for irradiation times longer than 50 ms, measurable intensity changes of the CH5 resonances were observed. Profiles of the percent NOE buildup versus irradiation time for $d(CG)_3T_4$ and $d(CG)_3$ in both 0.1 M NaCl and 4 M $NaClO_4$ were collected (data not shown). From the initial slopes of the buildup profiles, cross-relaxation rates for the CH5–CH6 vector, σ, were evaluated (Wagner & Wuthrich, 1979) as follows.

The NOE between protons i and j for short irradiation time is directly related to the cross-relaxation rate σ_{ij} by

$$\mathrm{NOE}_{ij}(t) \approx \sigma_{ij}t \qquad (5)$$

The measured cross-relaxation rate is related to the apparent correlation time τ_c (Soloman, 1955; Clore & Gronenborn, 1984) by

$$\sigma_{ij} = (\gamma^4\hbar^2/10r_{ij}^6)[\tau_c - 6\tau_c/(1 + 4\omega^2\tau_c^2)] \qquad (6)$$

ω is the spectrometer frequency, γ is the gyromagnetic ratio, and $\hbar$ is Planck's constant divided by 2π. Thus by knowing the interproton distance, r_{ij}, and cross-relaxation rate between the protons, the effective correlation time, τ_c, can be evaluated. In all calculations of τ_c (presented below and in Table II) a fixed length of 2.46 Å for the CH6–CH5 vector was assumed. Results of the analysis are summarized in Table II.

Comparison of the correlation times, corrected to the viscosity of water at 20 °C, in Table II reveals, in low salt when the duplex resides in the B conformation, the τ_c's for $d(CG)_3$ and $d(CG)_3T_4$ are nearly equivalent within experimental error (1.58 ns for the hairpin versus 1.85 ns for the linear duplex). In contrast, in high salt when the duplex resides in the Z conformation, $d(CG)_3$ has the longest correlation time of the set (τ_c = 1.91 ns), while $d(CG)_3T_4$ exhibits the shortest correlation time of the set (τ_c = 0.93 ns). Apparently, when the duplex stem resides in the B conformation, motions on the nanosecond time scale, on which τ_c directly depends, are only slightly affected by the T_4 end loop. This is definitely not the case when the duplex adopts the Z conformation, where motions on the nanosecond time scale are dramatically affected by the T_4 end loop and a 51% decrease in τ_c is induced by the presence of the loop.

Discussion

Recently a number of structural and thermodynamic studies on DNA oligomers of the general form $d(CG)_XT_Y(CG)_X$ with

(*X*, *Y*) = (2, 4), (3, 4), (5, 4), and (3, 5) have been reported (Xodo et al., 1986, 1988a,b; Germann et al., 1985; Hare & Reid, 1986; Ikuta et al., 1986; Wolk et al., 1988). Results of our studies of $d(CG)_3T_4$ and $d(CG)_3$ extend the already large data base on the structure and dynamics of self-complementary DNA oligomers of this type.

The results of this paper based on NMR and spectroscopic experiments of $d(CG)_3T_4$ and $d(CG)_3$ in high and low salt reveal (at least) five characteristics of the physical behavior of these DNAs. A brief discussion of each of these five features follows.

(1) The preferred conformation of $d(CG)_3T_4$ in either high or low salt is a unimolecular hairpin. In a previous study of $d(CG)_3T_4$ in a solvent of 0.1 M NaCl and 10 mM $NaHPO_4^-$, pH 6.0, electrophoretic, fluorescence polarization, and NMR data indicated this DNA oligomer exclusively forms an intramolecular hairpin in solution (Ikuta et al., 1986). The duplex stem region of the hairpin was found to form a right-handed B-type helix. Our finding that the self-complementary $d(CG)_3T_4$ adopts a unimolecular hairpin structure in 4 M $NaClO_4$ is consistent with similar findings on the similar self-complementary oligomer $d(CG)_5T_4(CG)_5$ in high salt (Germann et al., 1985; Wolk et al., 1988).

In solution, partially self-complementary oligomers of the type presently under discussion can conceivably form dimer-bulged duplex helices, monomer intramolecular hairpins, or a mixture of both conformers. However, of the molecules mentioned above for which studies have been reported, $d(CG)_3T_5(CG)_3$ alone displays a biphasic melting transition (Xodo et al., 1986, 1988a). The biphasic behavior for this heptadecamer persists in 0.1 M NaCl and 4.6 M $NaClO_4$. Structural features of the melting curve were shown to depend on DNA strand concentration over the range from 6 to 36 μM. This concentration range is within the DNA concentration range spanned in our optical melting study of $d(CG)_3T_4$ (5 and 500 μM). For $d(CG)_3T_5(CG)_3$ the low-temperature transition was shown to be concentration dependent with a t_m varying from 30 to 46 °C over the concentration range examined (Xodo et al., 1986). The higher temperature transition was found to be concentration independent in both low and high salt, although the t_m was about 20 °C lower in high salt. It was logically concluded that the low-temperature transition corresponds to dissociation of the bimolecular bulged duplex helices to unimolecular hairpins and the high-temperature transition arises from melting of the unimolecular hairpins to coiled single strands.

The published study of Hare and Reid (1986) showed over a wide range of DNA concentrations that $d(CG)_2T_4(CG)_2$ exclusively forms a unimolecular hairpin. In 0.1 M NaCl the melting curve of this oligomer is monophasic with t_m = 70 °C (Benight and Hare, unpublished data). Thus, deleting two base pairs from the stem of a duplex containing a T_4 hairpin loop on one end apparently destabilizes the hairpin toward melting by ~16 °C. The available body of data suggests formation of DNA hairpins with T_4 loops is favored over formation of the bulged duplex containing a T_8 internal loop. Interestingly, the studies of $d(CG)_3T_5(CG)_3$ (Xodo et al., 1986, 1988a,b) indicate formation of duplex helices containing 10 T's in a central bulge is favored over hairpins with T_5 loops. A justification for these observations can be provided entirely in terms of the length of the oligomers and the entropic contributions to the total free energy involved in formation of a hairpin loop versus a bulged duplex. Apparently a T_4 hairpin loop is favored over a bulged duplex loop containing eight unbound T residues. Alternatively, a bulged duplex containing 10 unbound T residues is apparently more entropically favorable than a T_5 hairpin loop. A formal description of these statements is given in terms of equilibrium statistical thermodynamics, under the umbrella of assumptions associated with the all-or-none model, in the Appendix.

(2) In high salt, the stem region of the hairpin is in a left-handed Z-type conformation. Studies of similar-sequence DNA hairpins having the stem in the left-handed Z conformation have been reported (Xodo et al., 1986, 1988b; Germann et al., 1985; Wolk et al., 1988). Recently, the first crystal structure of a DNA hairpin, formed by $d(CG)_3T_4$, indicated the duplex stem was in the Z conformation (Chattopadhyaya et al., 1988). Our CD and UV absorbance measurements concur with the crystallographic data. In high-salt solution, $d(CG)_3T_4$ also adopts the left-handed Z conformation.

NMR and CD studies of $d(CG)_5T_4(CG)_5$ in high- and low-salt conditions revealed the loop structure differs considerably depending on whether the duplex stem resides in the right-handed B or left-handed Z conformation (Wolk et al., 1988). In the crystal structure of $d(CG)_3T_4$ (Chattopadhyaya et al., 1988) the loop structure was also found to be considerably extended rather than inwardly stacked as reported for the solution structure proposed for $d(CG)_2T_4(CG)_2$ (Hare & Reid, 1986). A comparison of the solution structures of a T_4 loop nucleated by an alternating (CG) duplex stem in the Z conformation (Wolk et al., 1988) and in the B conformation (Hare & Reid, 1986) was made by Wolk et al. (1988). Our NOESY data of $d(CG)_3T_4$ in low and high salt, as far as they go, are in qualitative agreement with these previous observations and concur with the major conclusion that the structure of T_4 hairpin loops directly depends on the secondary structure of the duplex nucleating the loop.

(3) In either high or low salt, the hairpin is stabilized against melting by ~40 °C compared to the linear duplex. Published thermodynamic studies of the hairpin to single-strand transition in $d(CG)_3T_5(CG)_3$ (Xodo et al., 1986, 1988a) have evaluated the transition enthalpy and entropy of the hairpin oligomers and linear core duplex helices (Xodo et al., 1986, 1988a; Manzini et al., 1987). From these studies, effects of a T_5 hairpin loop on the stability of the duplex have been established. Employing a two-state analysis of the hairpin to single-strand transition of $d(CG)_3T_5(CG)_3$ (Xodo et al., 1988a), it was found the T_5 loop acts to slightly increase (by ~3 kcal/mol) the transition enthalpy, ΔH. Because the transition temperature of the hairpin was ~20 °C higher than that of the core linear duplex, the transition entropy, ΔS, which varies directly with ΔH and inversely with T_m, was found to be lower for the melting transition of the hairpin than for that of the core duplex. Therefore, the increased melting temperature of the hairpin formed by $d(CG)_3T_5(CG)_3$ is due to a slightly increased enthalpy of the core duplex stem by the T_5 loop and the greater entropic gain involved in melting the linear core duplex versus melting the hairpin. That is, the entropy of duplex nucleation is more favorable for complementary regions attached by noncomplementary residues (that comprise the loop after duplex nucleation) than for nucleating two individual complementary single strands that are free and unattached in solution. Comparison of ΔH evaluated from the melting curve of $d(CG)_3T_4$ with evaluated and published values of the core duplex $d(CG)_3$ indicates the transition enthalpies of the hairpin and $d(CG)_3$ in high and low salt are essentially identical. The ~40 °C higher T_m's observed for the hairpins over the core duplex in either salt indicates the greater stability of the hairpin is therefore entirely entropic in origin for the case of a T_4 loop.

(4) In high salt, as the temperature is elevated, the structural equilibrium of the duplex stem of the hairpin shifts from the Z to the B conformation prior to melting. A number of published studies of linear duplex DNA oligomers have reported a similar shift of the equilibrium from the Z to the B structure prior to denaturation (Holak et al., 1984; Tran-Dinh et al., 1984; Manzini et al., 1987; Quadrifoglio et al., 1981), an observation also reported for poly[d(GC)] in 2.5 M NaCl (Behe et al., 1985). No thermally induced shifts in the Z–B equilibrium were observed for the hairpin structure formed by $d(CG)_5T_4(CG)_5$ in 5 M NaCl (Germann et al., 1985) or $d(CG)_3T_5(CG)_3$ in 4.6 M $NaClO_4$ (Xodo et al., 1986). Our observations made in 4 M $NaClO_4$ indicate a small thermally induced shift of the equilibrium (~5 °C) from the Z to the B structure does occur in the stem of $d(CG)_3T_4$. Thus, both the duplex length and hairpin loop size apparently place constraints on the duplex sufficient to allow the Z to B transition of the hairpin.

(5) In low salt, when the DNA duplex exists in the B-conformation, attachment of a T_4 single-strand loop to one end only slightly decreases (by 14%) the correlation time, τ_c, of the CH5–CH6 interproton vector. In high salt, when the DNA duplex exists in the Z conformation, τ_c of the CH5–CH6 interproton vector decreases by 51%. These decreases in the correlation time of the CH5–CH6 interproton vector are taken to be indicative of increased motions of the duplex on the nanosecond time scale.

If we first assume that rotational tumbling in solution is the predominant relaxation mechanism on the nanosecond time scale in both the linear and hairpin DNAs, then the reduced τ_c values of the hairpins over the linear duplexes indicate the hairpins experience less rotational friction in solution. A reduced rotational friction factor for the hairpins necessarily implies a smaller hydrodynamic volume is occupied by them than by the linear core duplex. An estimate of the required volume reduction can be obtained by considering the dimensions of the hairpin and linear DNAs in the B and Z conformation. Assuming the inter base pair distance in B-DNA is 3.38 Å and in Z-DNA is 3.70 Å, the length of $d(CG)_3$ in is 20.28 Å in low salt and 22.20 Å in high salt. The hairpin loops are assumed to have a length of one base pair in low and high salt equivalent to the inter base pair length in that salt. Thus, the length of $d(CG)_3T_4$ is 23.66 Å in low salt and 25.90 Å in high salt. Diameters of the helix are assumed to be 24 Å in low salt and 20 Å in high salt. Hairpins and linear DNAs of these dimensions can be approximated as being roughly spherical. More sophisticated models considering the DNAs as spheroid cylinders of the dimensions given above result in friction factors for rotation parallel and perpendicular to the symmetry axis larger than or equal to those of spheres of equal volume (Yoshizaki & Yamakawa, 1980). Therefore, approximating the hairpins and core duplexes as spheres should provide a lower-limit estimate of the correlation times.

For a spherical particle, τ_c is given by

$$\tau_c = 8\pi\eta a^3/6k_BT \quad (7)$$

where a is the hydrodynamic radius of the sphere. In low salt a 14% reduction in hydrodynamic volume of the hairpin over that of the core duplex is required to account for the measured difference in τ_c. In high salt a 51% reduction in hydrodynamic volume of the hairpin over that of the core duplex is required. These required reductions in hydrodynamic volume correspond to a 5% decrease in the radius of the hairpin in low salt and 21% reduction in high salt of the hairpin radius over that of the linear core duplex. The reduction in radius obtained in low salt is very slight and probably not outside the experimental

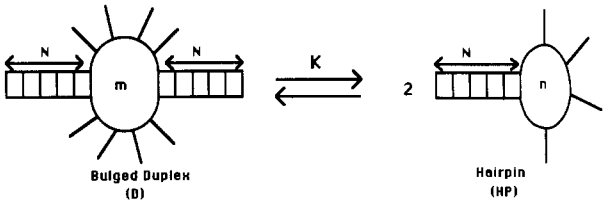

FIGURE 4

error and the error introduced by approximations involved in the calculation. The 21% radius reduction required for the hairpin in high salt is significant and appears to be physically unlikely, particularly in light of the extended loop structure of the hairpin in high salt (Chattopadhyaya et al., 1988; Wolk et al., 1988). Such a discrepancy casts doubt on the validity of our initial assumption, that overall tumbling in solution is the predominant relaxation mechanism accessible to the CH5–CH6 interproton vector on the nanosecond time scale. It is not known what the effect of the wobble motion introduced by the loop and associated asymmetry of the hairpin structure will be on the motions of the CH5–CH6 interproton vector, but it is presumed that the anisotropy of such motion should only increase the effective hydrodynamic volume of the molecule and thereby act to increase, not decrease, the rotational correlation time.

It is tempting to consider in the case of the Z hairpin that, in addition to overall tumbling, internal motions of the DNA duplex also substantially contribute to the relaxation process of the CH5–CH6 interproton vector. In this case, a substantially larger amplitude of this "internal motion" must persist in a Z-DNA than in a B-DNA duplex stem linked by a T_4 single-strand loop. A precise knowledge of the local modes of motion allowed in the CH5–CH6 interproton vector within the duplex helix environment and how the amplitudes of these motions are affected when the duplex is in the Z or B conformation is not available. This presently renders assignment of such motions as only qualitatively significant. Even so, this notion that a hairpin loop dramatically increases motions on the nanosecond time scale in Z-DNA while having virtually no effect on the motions of a B-DNA stem introduces a dynamic aspect to the relationship between Z-DNA and hairpin loops that warrants further study.

ACKNOWLEDGMENTS

We thank Drs. Steven Wolk and Ignacio Tinoco, Jr., for sending us their manuscript prior to publication.

APPENDIX

Hairpins versus Bulged-Loop Helices in Short Self-Complementary DNA Oligomers. We assume at a temperature well below the helix–coil transition temperature of either species an equilibrium between two species comprising the ensemble of self-complementary DNA strands. These are the bulged bimolecular duplex (D) and the self-bound unimolecular hairpin (HP) as shown in Figure 4. If we assume the transition state between the two species, which is not precisely known but believed to be the nonbonded single strand, is sufficiently short lived compared to the lifetime of either species (D or HP), then a two-state model can be employed to analyze the equilibrium between the two species. The two-state model has been employed in evaluating thermodynamic parameters for this type of reaction between short single-strand DNA oligomers (Xodo et al., 1986). The problem addressed here is precisely what factors determine the predominance of one species over the other or result in a mixture of the two. In this analysis the strictly two-state model is also employed.

The equilibrium between the species depicted in Figure 4 can be written as

$$D \overset{K}{\leftrightarrow} 2HP \tag{A1}$$

In equilibrium statistical thermodynamics the equilibrium constant K can be expressed in terms of the partition functions of the hairpin, $Z(HP)$, and bulged duplex, $Z(D)$, as

$$K = Z(HP)^2/Z(D) = Z_{int}(HP)^2 Z_{ext}(HP)^2/Z_{int}(D)Z_{ext}(D) \tag{A2}$$

$Z_{int}(HP)$, $Z_{int}(D)$, $Z_{ext}(HP)$, and $Z_{ext}(D)$ are the partition functions for the internal and external degrees of freedom of D and HP. For the internal degrees of freedom, the partition functions can be expressed in terms of parameters of the familiar DNA helix–coil transition theory (Benight et al., 1981; Wartell & Benight, 1985). For the all-or-none model only one conformational state is accessible to the hairpin or bulged duplex. Therefore, the partition functions are merely the statistical weights for the respective species. If we arbitrarily choose the free-energy standard state as the nonbonded single strand, then

$$Z_{int}(HP) = \prod_{i}^{N} s_i f_{end}(n)\sigma^{1/2} \tag{A3}$$

$$Z_{int}(D) = \prod_{i}^{2N} s_i f_{int}(m)\sigma \tag{A4}$$

s_i is the stability parameter for each base pair that includes the free energy involved in forming a base-pair complex in either a hairpin stem or bimolecular duplex region. σ is the cooperativity parameter that accounts for the stacking interactions that must be established in closing a loop. For the hairpin, a factor of $\sigma^{1/2}$ is assigned since only one stacking interaction must be established to form a hairpin loop. Formation of an internal loop in a duplex requires the establishment of two stacking interactions; therefore, a factor of σ appears in the statistical weight. As given, $\sigma^{1/2}$ is the average cooperativity parameter for all types of base pairs and does not explicitly include nearest-neighbor interactions. $f_{end}(n)$ is the loop entropy function for forming a hairpin or end loop containing n single strand residues. $f_{int}(m)$ is the loop entropy function for forming an internal loop of m base pairs sandwiched between duplex regions. $f_{end}(n)$ and $f_{int}(m)$ originate from the treatment of Jacobson and Stockmayer (1950) on the probability of self-interaction of a multiple-link random flight chain. The relationship between $f_{end}(n)$ and $f_{int}(m)$ has been recently discussed (Benight et al., 1988).

From earlier work (Poland & Scheraga, 1970; Benight et al., 1981; Hillen et al., 1981; Wartell & Benight, 1985), the ratio of the partition functions of the external degrees of freedom is defined as

$$\beta \equiv Z_{ext}(D)/Z_{ext}(HP)^2 \tag{A5}$$

β is the nucleation parameter and accounts for the relative difficulty of forming the first base pair of a bimolecular duplex from two single strands, compared to the formation of the remaining base pairs subsequent to formation of the first base pair. With these definitions the equilibrium constant for the reaction in eq A1 becomes

$$K = f_{end}(n)^2/f_{int}(m)\beta \tag{A6}$$

Thus the equilibrium constant depends only on the relative probability of hairpin versus internal loop formation and duplex nucleation parameter, β.

Estimates of β can be made by realizing that the external partition functions of D and HP depend on the translational and rotational partition functions of D and HP which in turn are determined by the translational and rotational moments of inertia of HP and D. The translational and rotational moments of inertia are determined by the mass of the hairpin and bulged duplex and therefore directly depend on the number of base pairs comprising the hairpin or bulged duplex. Thus, the expression for β can be rewritten in terms of the number of base pairs in the HP, N, as (Poland & Scheraga, 1970; Benight et al., 1981)

$$\beta = C(2N)^{a_1}/(N^{a_2})^2 = C'N^{\alpha} \tag{A7}$$

C and C' are proportionality constants that include all factors independent of N. The value of the exponent, $\alpha = a_1 - 2a_2$, is determined by the mass dependence of the translational and rotational partition functions of the hairpin and bulged duplex. The translational partition functions, Z_{tran}, vary as $M^{3/2}$ independent of the shape of the molecules. The rotational partition functions, Z_{rot}, vary differently with the mass of the molecules depending on their shape. For example, a rod-like molecule has Z_{rot} proportional to $M^{7/2}$ while for a spherical molecule Z_{rot} goes like $M^{5/2}$. Thus, for an equilibrium of rod-like bulged-duplex helices dissociating to two sphere-like single-strand hairpins, α in eq A7 is -3. If the equilibrium is modeled as a sphere-like duplex dissociating to two sphere-like hairpins, $\alpha = -4$. In any case under consideration, β should not be greater than 1. All published estimates of β, including those resulting from the above analysis, indicate $\beta < 10^{-2}$ (Applequist & Damle, 1963; Scheffler et al., 1970; Benight et al., 1981; Hillen et al., 1981; Wartell & Benight, 1985).

Recently, $f_{end}(n)$ was evaluated for a T_4 loop closed by a C-G base pair in a heterogeneous-sequence self-complementary DNA minicircle (Benight et al., 1988):

$$f_{end}(n) = ML/(n + 1)^{1.5} \tag{A8}$$

For a T_4 end loop, the loop weighting parameters reported were $M = 2.03$ and $L = 44$, yielding $f_{end}(4) = 7.99$. More recent work on $d(CG)_3T_4$ indicates $f_{end}(4)$ is approximately 10-fold smaller in the alternating sequence hairpin than in the dumbbell (T. M. Paner and A. S. Benight, unpublished results). Thus, we employ $f_{end}(4) = 0.89$. An empirical form of $f_{int}(m)$, more appropriate for small internal loops, has also been reported (Wartell & Benight, 1985; Wartell, 1977):

$$f_{int}(m) = 1/(1 - 1.38^{-0.1m})(m + 1)^{1.7} \tag{A9}$$

Thus, for $m = 4$, $f_{int}(4) = 0.54$. With these available estimates of $f_{end}(4)$ and $f_{int}(4)$, the equilibrium constant, K, for the duplex to hairpin dissociation reaction as given in eq A6 is evaluated to be

$$K = 0.79/0.54\beta = 1.46/\beta \tag{A10}$$

Since $\beta \ll 1$, $K \gg 1$. Therefore, the free-energy change in the duplex to hairpin reaction is negative, and the equilibrium lies far to the right. Consequently, only unimolecular hairpins are present in the solution.

This analysis can similarly be employed to account for the observations reported for self-complementary DNA oligomers containing five unbound T residues. Recall for T_5 loops, the bulged bimolecular species predominates over the unimolecular hairpins (Xodo et al., 1986, 1988a). Apparently, in this case, in contrast to that found for internal loops containing eight T residues versus T_4 hairpin loops, the free energy for forming an internal loop of 10 unbound T residues is lower than twice the free-energy of forming a T_5 hairpin loop. However, a semiquantitative verification for this proposition is not possible at this time for the T_5 loops since no reliable estimates of $f_{end}(5)$

are currently available. Evaluations of these loop entropy functions, based on analysis of melting curves of bulged duplexes and hairpins containing varying numbers of single-strand residues in their loops, with the exact equilibrium statistical mechanical theory of DNA melting are currently under way (Benight et al., unpublished results). For equilibria that deviate substantially from two-state behavior, the analysis can be extended to rigorously include all equilibrium microstates of the bulged duplex and hairpin species contributing to the equilibrium constant. In this case the partition functions in eq A3 and A4 for each species are sums over the statistical weights of all possible microstates of the duplex and hairpin species.

Registry No. d(CGCGCGTTTTCGCGCG), 102419-87-4; d(CGCGCG), 58927-26-7.

References

Antosiewicz, J., Germann, M. W., van de Sande, J. H., & Porschke, D. (1988) *Biopolymers 27*, 1319–1327.

Applequist, J., & Damle, V. (1965) *J. Am. Chem. Soc. 87*, 1450–1458.

Behe, M., Felsenfeld, G., Szu, S., & Charney, E. (1985) *Biopolymers 24*, 289–300.

Benight, A. S., Wartell, R. M., & Howell, D. K. (1981) *Nature (London) 289*, 203–205.

Benight, A. S., Schurr, J. M., Flynn, P. F., Reid, B. R., & Wemmer, D. E. (1988) *J. Mol. Biol. 200*, 377–399.

Caruthers, M. H. (1982) in *Chemical and Enzymatic Synthesis of Gene Fragments. A Laboratory Manual* (Gassen, H. G., & Lang, A., Eds.) pp 71–79, Verlag-Chemie, Weinheim, FRG.

Chattopadhayaya, R., Ikuta, S., Grzeskowiak, K., & Dickerson, R. E. (1988) *Nature (London) 334*, 175–179.

Clore, G. M., & Gronenborn, A. M. (1984) *FEBS 172*, 219–225.

Germann, M. W., Schoenwaedler, K., & van de Sande, J. H. (1985) *Biochemistry 24*, 5698–5702.

Gonzalez, A., Talavera, A., Almendral, J. M., & Vinuela, E. (1986) *Nucleic Acids Res. 14*, 6835–6844.

Haasnoot, C. A. G., den Hartog, J. H. J., de Rooij, J. F. M., van Boom, J. H., & Altona, C. (1980) *Nucleic Acids Res. 8*, 169–181.

Haasnoot, C. A. G., de Bruin, S. H., Brendsen, R. G., Janssen, H. G. J. M., Binnendiik, T. J. J., Hilbers, C. W., van der Marel, G. A., & van Boom, J. H. (1983) *J. Biomol. Sterodyn. 1*, 115–129.

Haniford, D. B., & Pulleyblank, D. E. (1985) *Nucleic Acids Res. 13*, 4343–4363.

Hare, D. R., & Reid, B. R. (1986) *Biochemistry 25*, 5341–5350.

Hillen, W., Goodman, T. C., Benight, A. S., Wartell, R. M., & Wells, R. D. (1981) *J. Biol. Chem. 256*, 2761–2766.

Hobom, G., Grosschedl, R., Lusky, M., Scherer, G., Schwarz, E., & Kossel, H. (1978) *Cold Spring Harbor Symp. Quant. Biol. 43*, 165–178.

Holak, T. A., Borer, P. N., Levy, G. C., van Boom, J. H., & Wang, A. H. J. (1984) *Nucleic Acids Res. 12*, 4625–4635.

Ikuta, S., Chattopadhyaya, R., & Dickerson, R. E. (1984) *Anal. Chem. 56*, 2253–2256.

Ikuta, S., Chattopadhyaya, R., Dickerson, R. E., & Kearns, D. R. (1986) *Biochemistry 25*, 4840–4849.

Jacobson, H., & Stockmayer, W. H. (1950) *J. Chem. Phys. 18*, 1600–1608.

Kim, S. H., Quigley, G., Suddath, F. L., McPherson, A., Sneden, D., Kim, J. J., Weinzer, J., & Rich, A. (1973) *J. Mol. Biol. 75*, 421–428.

Kleckner, N., Chan, R. K., Ty, B. K., & Botstein, D. (1975) *J. Mol. Biol. 97*, 561–575.

Lilley, D. M. J. (1980) *Proc. Natl. Acad. Sci. U.S.A. 77*, 6468–6472.

Maniatis, T., Ptashne, M., Backman, K., Kleid, D., Flashman, S., Jeffrey, A., & Maurer, R. (1975) *Cell 5*, 109–113.

Manzini, G., Xodo, L. E., Quadrifoglio, F., van Boom, J. H., & van der Marel, G. A. (1987) *J. Biomol. Struct. Dyn. 4*, 651–662.

Marky, L. A., Blumenfeld, K. S., Kozlowski, S., & Breslauer, K. J. (1983) *Biopolymers 22*, 1247–1257.

Muller, U. R., & Fitch, W. M. (1982) *Nature (London) 289*, 582–585.

Nadeau, J. D., & Gilham, P. T. (1985) *Nucleic Acids Res. 13*, 8259–8274.

Panayotatos, N., & Wells, R. D. (1981) *Nature (London) 289*, 466–470.

Patel, D. J., Kozlowski, S. A., Nordheim, A., & Rich, A. (1982) *Proc. Natl. Acad. Sci. U.S.A. 79*, 1413–1417.

Petersheim, M., & Turner, D. H. (1983) *Biochemistry 22*, 269–277.

Poland, D., & Scheraga, H. A. (1970) *Theory of Helix-Coil Transitions in Biopolymers*, Academic Press, New York.

Quadrifoglio, F., Manzini, G., Vasser, M., Dinkelspeil, K., & Crea, R. (1981) *Nucleic Acids Res. 12*, 2195–2206.

Quigley, G. J., & Riche, A. (1976) *Science 194*, 796–806.

Rosenberg, M., & Court, D. (1979) *Annu. Rev. Genet. 13*, 319–353.

Roy, S., Weinstein, S., Borah, B., Nickol, J., Apella, E., Sussman, J., Miller, M., Shindo, H., & Cohen, J. S. (1986) *Biochemistry 25*, 7417–7423.

Scheffler, I. E., Elson, E. L., & Baldwin, R. L. (1970) *J. Mol. Biol. 48*, 145–171.

Soloman, I. (1955) *Physiol. Rev. 99*, 559–565.

States, D. J., Haberkorn, R. A., & Rubin, D. J. (1982) *J. Magn. Reson. 48*, 286–292.

Summers, M. F., Byrd, R. A., Gallo, K. A., Samson, C. J., Zon, G., & Egan, W. (1985) *Nucleic Acids Res. 13*, 6375–6386.

Tan, Z.-K., Ikuta, S., Huang, T., Dugaiczyk, A., & Itakura, K. (1983) *Cold Spring Harbor Symp. Quant. Biol. 47*, 383–391.

Tran-Dinh, S., Taboury, J., Neumann, J. M., Tam, H. D., Genissel, B., Langlois d'Estaintot, B., & Igolen, J. (1984) *Biochemistry 23*, 1362–1371.

Vologodskii, A. V., Lukashin, A. V., Anshelevich, V. V., & Frank-Kamenetskii, M. D. (1979) *Nucleic Acids Res. 6*, 967–982.

Wagner, G., & Wutrich, K. (1979) *J. Magn. Reson. 33*, 675–680.

Wartell, R. M. (1977) *Nucleic Acids Res. 4*, 2779–2797.

Wartell, R. M., & Benight, A. S. (1985) *Phys. Rep. 126*, 67–107.

Wells, R. D., Goodman, T. C., Hillen, W., Horn, G. T., Klein, R. D., Larson, J. E., Muller, U. R., Neuendorf, S. K., Panayotatos, N., & Stirdivant, S. M. (1980) *Prog. Nucleic Acid Res. Mol. Biol. 25*, 167–267.

Wemmer, D. E., Chou, S. H., Hare, D. R., & Reid, B. R. (1985) *Nucleic Acids Res. 13*, 3755–3772.

Wolk, S., Hardin, C. C., Germann, M. W., van de Sande, J. H., & Tinoco, I., Jr. (1988) *Biochemistry 27*, 6960–6967.

Xodo, L. E., Manzini, G., Quadrifoglio, F., van der Marel, G. A., & van Boom, J. H. (1986) *Nucleic Acids Res. 14*, 5389–5398.

Xodo, L. E., Manzini, G., Quadrifoglio, F., van der Marel, G. A., & van Boom, J. H. (1988a) *Biochemistry 27*, 6321–6326.
Xodo, L. E., Manzini, G., Quadrifoglio, F., van der Marel, G. A., & van Boom, J. H. (1988b) *Biochemistry 27*, 6327–6331.
Yoshizaki, T., & Yamakawa, H. (1980) *J. Chem. Phys. 72*, 57–69.
Zurawski, G., Elseviers, D., Stauffer, G. V., & Yanofsky, C. (1978) *Proc. Natl. Acad. Sci. U.S.A. 75*, 5988–5992.

Sodium-23 NMR Spin–Lattice Relaxation Rate Studies of Mono- and Bis-Intercalation in DNA

Hanne Eggert

Chemical Laboratory II, The H. C. Ørsted Institute, University of Copenhagen, Universitetsparken 5, DK-2100 Copenhagen Ø, Denmark

Jørgen Dinesen and Jens Peter Jacobsen*

Department of Chemistry, Odense University, Campusvej 55, DK-5230 Odense M, Denmark

Received September 8, 1988; Revised Manuscript Received November 30, 1988

ABSTRACT: ^{23}Na spin–lattice relaxation rate ($1/T_1 = R_1$) measurements have been used to study the intercalation of a series of 9-aminoacridine derivatives in DNA. The ^{23}Na relaxation rate is strongly dependent upon the amount of intercalator added to a sodium DNA solution. The results are analyzed by a combined use of the ion condensation theory and the quadrupolar relaxation theory of polyelectrolyte solutions. This interpretation shows that the major effect in lowering the relaxation rate by intercalation is not due to the release of sodium ions but is caused by a substantial decrease in the relaxation rate R_b for the remaining bound sodium ions. Likewise, titration of NaDNA solutions with $MgCl_2$ shows that condensation of Mg^{2+} on the DNA double helix reduces R_b. A good agreement between experiment and theory is found if the average lengthening following intercalation of a 9-aminoacridine moiety is assumed to be approximately 2.7 Å. The distinction between mono- and bis-intercalation is clearly indicated by the results. The two bis-intercalating drugs examined are found to bis-intercalate only up to $r \leq 0.02$. For $r > 0.02$ the drugs apparently mono-intercalate.

The overall conformation and physical properties of DNA in solution are strongly influenced by association with counterions, e.g., Na^+. Sodium-23 NMR spectroscopy has been applied in several studies of DNA. Association of sodium and other simple cations to DNA in solution has been examined by using ^{23}Na line width measurements (Andersen et al., 1978; Bleam et al., 1980, 1983; Mariam & Wilson, 1983; Nordenskjold et al., 1984; Braunlin et al., 1986; Delville et al., 1986). Recently, T_1 spin relaxation measurements have been introduced in the investigations (Nordenskjold et al., 1984; Delville et al., 1986).

Intercalation is one of several modes whereby drugs interact with DNA. A planar part of the drug is inserted in between adjacent stacked base pairs of a double-stranded DNA. The intercalation process results in a helix extension. This increases the average phosphate to phosphate distance and decreases thereby the DNA charge density. Positive charges on the intercalator neutralize some of the anionic charge of DNA, which also reduces the charge density. Counterions, e.g., Na^+, are associated (called bound) to the DNA to stabilize the helix structure. The intercalation process will reduce the relaxation rate of the bound Na^+ due to the charge density reduction and hindrance of DNA internal motion. Furthermore, the charge density reduction results in a release of bound Na^+. These effects strongly influence the spin relaxation rates of ^{23}Na measured by NMR spectroscopy.

Mariam and Wilson (1983) have studied the intercalation of ethidium bromide in DNA by using ^{23}Na NMR line width measurements. A dramatic decrease of the line width upon intercalation was found. Several problems arise when ^{23}Na line widths are used as the relaxation parameter. Non-Lorentzian line shapes may appear due to the spin dynamical behavior of spin $I = {}^3/_2$ nuclei. Furthermore, line broadening caused by intermediate fast exchange between free and bound sodium ions cannot be excluded together with line shape effects created by the presence of medium-range order in the DNA solution (H. Eggert, J. Dinesen, and J. P. Jacobsen, unpublished results). Although spin dynamics also complicate spin–lattice relaxation (T_1) behavior, an average T_1 spin relaxation time can be obtained independently of the exchange phenomena. The field dependency of ^{23}Na T_1 in DNA solution indicates that the bound sodium ions are in intermediate motional narrowing range (Eggert et al., unpublished results), and relaxation can therefore be treated as single exponential (Bull, 1972). These facts have prompted us to use T_1 relaxation measurements instead of line width measurements to follow intercalation processes.

The intercalation mode of binding was first proposed by Lerman (1961) for binding of aminoacridines to DNA. Since then, intercalation of this class of compounds has been widely studied by several methods (Le Pecq et al., 1975; Wakelin et al., 1978; Wright et al., 1980; Assa-Munt et al., 1985; Wirth et al., 1988). Compounds containing two aminoacridine functional groups joined by a molecular linker chain are po-

* Author to whom correspondence should be addressed.

0006-2960/89/0428-3332$01.50/0